CrossMark

Stanisław D. Głazek · Patryk Kubiczek

Proton Structure in High-Energy High-Multiplicity p–p Collisions

Abstract A few-body proton image, expected to be derivable from QCD in the renormalization group procedure for effective particles, is used within the Monte Carlo Glauber model to calculate the anisotropy coefficients in the initial collision-state of matter in high-energy high-multiplicity proton–proton interaction events. We estimate the ridge-like correlations in the final hadronic state by assuming their proportionality to the initial collision-state anisotropy. In our estimates, some distinct few-body proton structures appear capable of accounting for the magnitude of p–p ridge effect, with potentially discernible differences in dependence on multiplicity.

1 Introduction

Protons resist precise theoretical description of their internal dynamics in the Minkowski space–time for a long time by now. The simplest such picture, which is provided by the constituent quark model used to classify hadrons, is not precisely derived from QCD. The theory itself uses the Euclidean-space techniques that do not easily yield any real space–time image. In these circumstances, it is of interest to note that high-energy high-multiplicity proton–proton (pp) collisions may shed new light on the issue of proton structure. Namely, the numerous products in such collisions exhibit collective behavior that appears dependent on the initial state of colliding proton matter and the latter depends on the proton structure. Thus, the correlations among products in high-energy high-multiplicity pp collisions may report on the proton structure.

In particular, the CMS [1] and ATLAS [2] collaborations reported the collective flow in pp collisions that resembles the one observed in heavy-ion collisions [3–5]. Several authors discussed such flows in pp collisions [6–18] and we follow the insights of Ref. [6] in order to estimate the extent to which the high-energy high-multiplicity pp events are sensitive to the model of proton structure. Following the approach of Ref. [6] and the parameter choice such as in Ref. [15], used here, means making a strong assumption that the parton medium produced in the overlap region of pp collision at the LHC has similar hydrodynamical properties as that in heavy ion collisions at RHIC. The individual proton structures we consider are motivated by the general features of the renormalization group procedure for effective particles (RGPEP) in quantum field theory [19,20].

We find that, the effective picture of a quark and diquark with a gluon flux between them produces a different dependence of eccentricity and triangularity on multiplicity than the three-quark picture with a star-like junction

S. D. Głazek (✉)
Institute of Theoretical Physics, Faculty of Physics, University of Warsaw, Pasteura 5, 02-093 Warsaw, Poland
E-mail: stglazek@fuw.edu.pl

P. Kubiczek
Faculty of Physics, Astronomy and Applied Computer Science, Jagiellonian University, Łojasiewicza 11, 30-348 Kraków, Poland
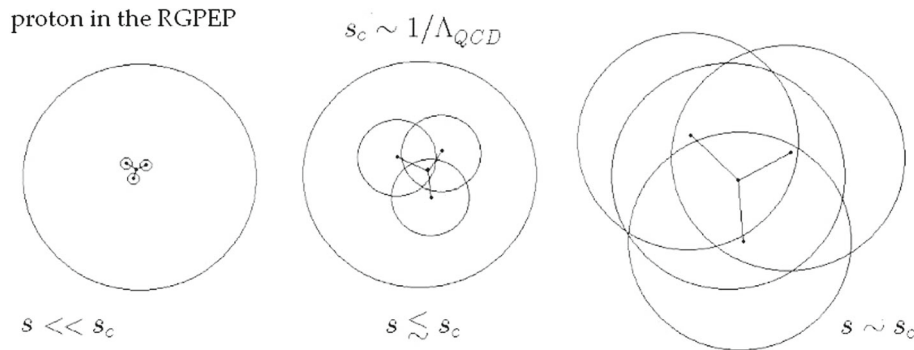E-mail: patryk.kubiczek@gmail.com

Fig. 1 Proton structure described using effective quarks of size s that is very much smaller than, smaller and comparable with the constituent quark size s_c, with the single large circle indicating the volume available for effective gluons irrespective of their corresponding size, see Ref. [19]

made of gluons does. According to this finding, the recent data for high-energy high-multiplicity events suggest a significant star-like gluon junction component in the proton structure. Our analysis also indicates a need for assessing the adequacy of the linear relationship used by us between asymmetries in the initial collision state, such as the eccentricity or triangularity, and the final state correlations in high-multiplicity events, such as the elliptic flow.

2 Proton Structure in *pp* Collisions

As mentioned in Sect. 1, the ridge-effect in *pp* scattering can be described using the hydrodynamic evolution of the asymmetric state of matter that results from one proton's quark and gluon distribution suddenly colliding with another's. The asymmetric state is meant to evolve according to laws of hydrodynamics until it eventually turns into the detected particles that emerge through hadronization in the final state, in which they exhibit the angular correlation over a long-range in rapidity, called the ridge. The final state ridge-like correlations, such as the elliptic flow, are thus related to the initial stage of *pp* collision whose nature depends on the proton structure. One of the key issues is thus how to describe the proton structure using QCD in the Minkowski space–time.

Conceptually, we approach this issue using the RGPEP [19,20], which is a candidate for providing the mathematical tools for describing protons as bound states of effective quarks and gluons of specific size s. The size parameter s plays the role of an arbitrary renormalization-group scale that can be adjusted to the physical process one wants to accurately describe in simplest possible terms. This condition means choosing the right variables for grasping the essence of physics most economically from the computational point of view. The scale dependence of the proton structure expected in the RGPEP is illustrated in Fig. 1 and the corresponding examples of the color structure are shown in Fig. 2. The expectation is based on the scale-dependent features of effective Hamiltonians, which imply the possibility that a relativistic bound-state eigenvalue problem can be equivalently written in terms of a few-body problem for sizable effective quarks and gluons instead of an infinite combination of bare point-like quarks and gluons of canonical QCD. Hence, the RGPEP provides the scheme in which the distribution of matter in proton can be imagined in terms of wave functions, or probability distributions for the effective quarks and gluons of size s.

The few-body picture of protons in QCD suggested by the RGPEP allows us to preliminarily model the proton structure in terms of shapes illustrated by two typical examples in Fig. 3 [21], knowing that such models can in future be verified in theory. We ask if the ridge effect can phenomenologically distinguish between the effective configurations.

We consider three types of configurations. The proton quark–diquark configuration, denoted by **I** and shown on the left-hand side of Fig. 3, is motivated by Refs. [17,18]. It is a superposition of a few Gaussians that represent a quark, a diquark and gluons forming a tube in between. The three-quark configuration, denoted by **Y** and shown on the right-hand side of Fig. 3, is motivated by Ref. [19]. It is a superposition of Gaussians that represent three quarks and additional gluons forming the Y-shaped junction. The shape of **Y** configuration is kept fixed. In addition, we consider the Gaussian fluctuating three-quark configuration, denoted by **G–f**, which
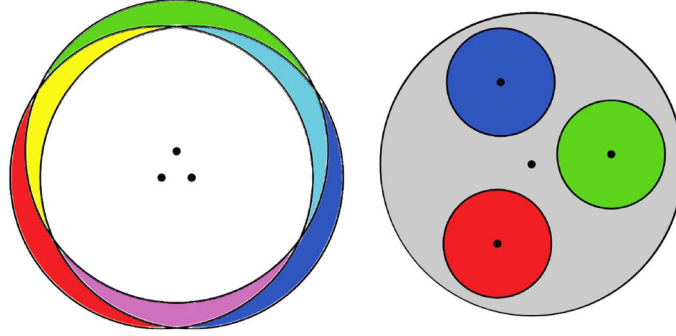
Fig. 2 *Color* structure of effective quarks for two values of the RGPEP scale parameter $s \sim s_c$ and $s < s_c$ in Fig. 1. Pions are meant to couple to nucleons in the constituent quark picture only at the nucleon boundaries, where *color* is not neutralized, and for smaller values of s the quarks form more localized objects with the gray area indicating the volume available for effective gluons of a similar size to the quarks (drawing from Ref. [22]) (color figure online)
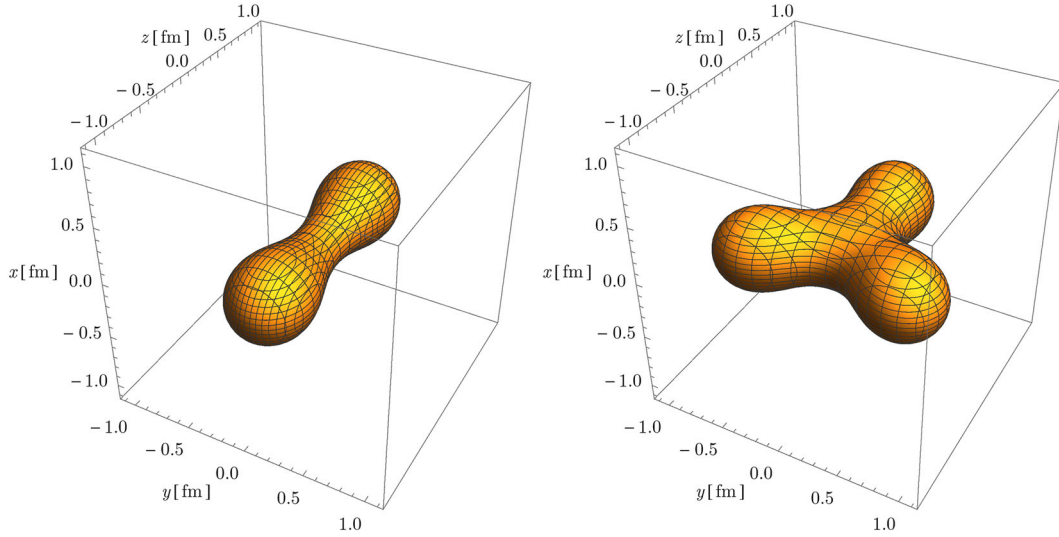

Fig. 3 Effective constituent configurations of typical size s in proton: on the *left* is the quark–diquark configuration labeled in the text as **I** and on the *right* is the three-quark configuration with a star-junction built from gluons labeled in the text by **Y**

is the same as the **Y** configuration but with the shape parameters generated according to Gaussian probability distributions. Details of all configurations we consider are available in Refs. [21,22].

3 Asymmetries in the Initial Stage of a *pp* Collision and the Final State Correlations

Following Ref. [6], we adapt a simple Glauber model, widely used for modelling high energy nuclear collisions [23], to describe the density of binary partonic collisions in scattering of two systems A and B,

$$
n_{\text{coll}}(x, y; b, \boldsymbol{\Sigma}_A, \boldsymbol{\Sigma}_B) = \sigma_{gg} \int\limits_{-\infty}^{\infty} dz\, \rho\left(x - \frac{b}{2}, y, z; \boldsymbol{\Sigma}_A\right) \int\limits_{-\infty}^{\infty} dz'\, \rho\left(x + \frac{b}{2}, y, z'; \boldsymbol{\Sigma}_B\right), \tag{1}
$$

which is a function of the coordinates x and y in the plane transverse to the colliding beams, the impact parameter b and the varying parameters $\boldsymbol{\Sigma}$ that identify the proton structure and its orientation in space. The coefficient σ_{gg} denotes a parton–parton scattering cross-section, in our estimates on the order of 4 mb, and ρ denotes the three-dimensional parton distribution described in Sect. 2.

Eccentricity ϵ_2 and triangularity ϵ_3 in the initial stage of pp collision are calculated using the formula [24]

$$\epsilon_n = \frac{\sqrt{\{s^n \cos(n\phi)\}^2 + \{s^n \sin(n\phi)\}^2}}{\{s^n\}}, \tag{2}$$

in which the curly brackets denote the expectation value

$$\{f(x, y)\} = \frac{\int dx\, dy\, f(x, y)\, n_{\text{coll}}(x, y; b, \mathbf{\Sigma}_A, \mathbf{\Sigma}_B)}{\int dx\, dy\, n_{\text{coll}}(x, y; b, \mathbf{\Sigma}_A, \mathbf{\Sigma}_B)}, \tag{3}$$

and coordinates are parameterized as $x = s \cos \phi$, $y = s \sin \phi$. The number of collisions in an event is

$$N_{\text{coll}}(b, \mathbf{\Sigma}_A, \mathbf{\Sigma}_B) = \int dx\, dy\, n_{\text{coll}}(x, y; b, \mathbf{\Sigma}_A, \mathbf{\Sigma}_B) \tag{4}$$

and the cross-section density in the impact parameter plane is

$$\sigma(b, \mathbf{\Sigma}_A, \mathbf{\Sigma}_B) = 1 - \left[1 - \frac{N_{\text{coll}}(b, \mathbf{\Sigma}_A, \mathbf{\Sigma}_B)}{N_g^2}\right]^{N_g^2}. \tag{5}$$

The total pp cross-section is thus

$$\sigma_{pp} = \int\limits_0^\infty 2\pi b\, db \int P(\mathbf{\Sigma}_A)\, d\mathbf{\Sigma}_A \int P(\mathbf{\Sigma}_B)\, d\mathbf{\Sigma}_B\, \sigma(b, \mathbf{\Sigma}_A, \mathbf{\Sigma}_B), \tag{6}$$

where $P(\mathbf{\Sigma})$ is the probability density for proton configuration $\mathbf{\Sigma}$. For any quantity Q, its expectation value in many collisions is

$$\langle Q \rangle = \frac{1}{\sigma_{pp}} \int\limits_0^\infty 2\pi b\, db \int P(\mathbf{\Sigma}_A)\, d\mathbf{\Sigma}_A \int P(\mathbf{\Sigma}_B)\, d\mathbf{\Sigma}_B\, \sigma(b, \mathbf{\Sigma}_A, \mathbf{\Sigma}_B)\, Q(b, \mathbf{\Sigma}_A, \mathbf{\Sigma}_B). \tag{7}$$

We used randomly oriented proton configurations in the Monte Carlo generation of about $3 \cdot 10^5$ events for each proton model and estimated the averaged eccentricity ϵ_2 and triangularity ϵ_3 in the resulting samples. In our estimates, $\sigma_{gg} \sim 4.3\,\text{mb}$ [15] and $\sigma_{pp} \sim 60\,\text{mb}$ [25] required the number of scattering partons $N_g = 9 \pm 2$ to obtain agreement with data, assuming that the multiplicity $N = \alpha N_{\text{coll}}$ and reproducing the value $\langle N \rangle = 30$ [26] for charged particles by choosing $\alpha = 8 \pm 3$. Our minimum bias results for eccentricity and triangularity are shown in Fig. 4

It is visible in Fig. 4 that the initial stage of pp collision is characterized by different multiplicity dependence of the asymmetries for different proton structures. In collisions of quark–diquark (**II**) and Gaussian-fluctuating (**G–f**) structures, the asymmetries decrease with multiplicity above about $N = 100$, while in the collisions of tripod three-quark configurations (**YY**) the initial stage asymmetries persist or even increase above $N = 100$.

In order to relate the eccentricity and triangularity to data, we note that the observable multiplicity distributions in transverse momentum p_T and pseudorapidity η are conventionally written as

$$\frac{d^3 N}{d^2 p_T d\eta} = \left\{1 + 2 \sum_{n=1}^\infty v_n(p_T, \eta) \cos[n(\phi - \Phi_{RP})]\right\} \frac{d^2 N}{2\pi p_T dp_T d\eta}, \tag{8}$$

where the reaction plane angle Φ_{RP} for colliding spherically symmetric distributions is illustrated in Fig. 5. In the actual events the angles Φ_{RP} are determined from the particle distributions.

Assuming that the averaged minimal bias elliptic flow parameter v_2 is proportional to the minimal bias eccentricity parameter ϵ_2 with coefficient order 0.3 [15], we obtain $v_2 \sim 0.11$, 0.14 and 0.09 for the proton models **II**, **YY** and **G–f**, respectively, while data indicates v_2 in the range 0.04–0.08 [5].

More generally, taking into account that the initial-stage asymmetry parameters ϵ_n in Eq. (2) and the final-state coefficients v_n in Eq. (8) are small, and assuming that a set of averaged coefficients v_n with different n depends approximately linearly on the set of averaged parameters ϵ_n, one can infer the dependence of v_n on
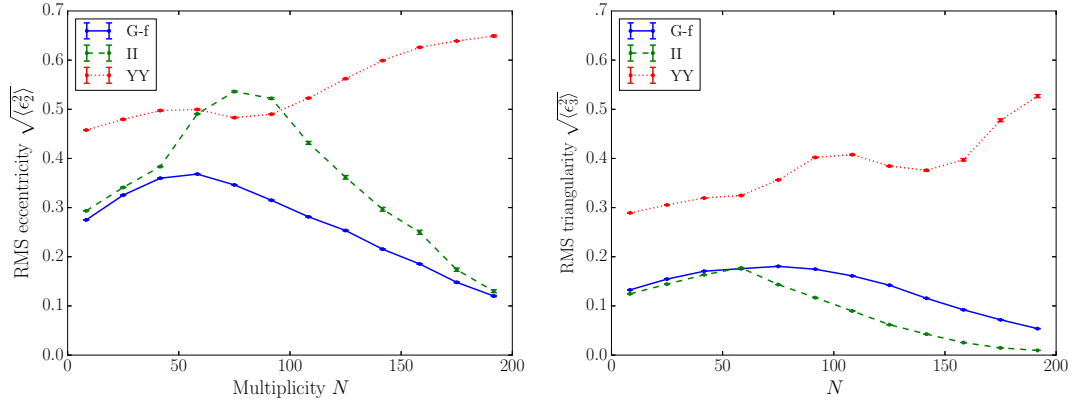
Fig. 4 Average eccentricity and triangularity obtained using Eq. (7) for three different types of proton structure in pp collisions. Green curves labeled **II** correspond to collisions of protons in configuration **I** in Fig. 3, and the red curves labeled **YY** correspond to collisions in configurations **Y** in Fig. 3. The *blue lines* labeled **G–f** correspond to the Gaussian fluctuating three-quark configuration in which the **Y**-type proton configurations appear with different shape parameters according to a Gaussian probability distribution [21]. Note the distinct multiplicity dependence in the case of **YY** configurations (color figure online)
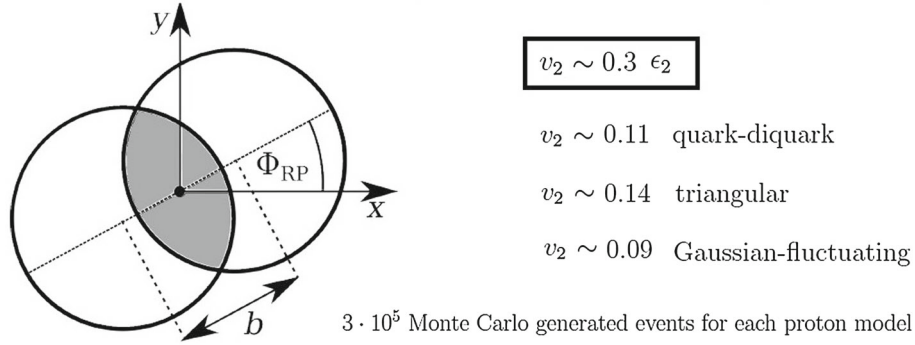

Fig. 5 View of the initial stage of pp collision along the beam for illustration of Eq. (8). The average value of the elliptic flow coefficient $v_2(p_T, \eta)$, denoted by v_2, is assumed to be proportional to the eccentricity $\sqrt{\langle \epsilon_2^2 \rangle}$ obtained in Eq. (7) with a coefficient on the order of 0.3 [15]. The magnitudes of v_2 resulting from different proton models are displayed with quark–diquark = **II**, triangular = **YY**

multiplicity N from the dependence of ϵ_n on N. Accordingly, Fig. 4 suggests that the averaged elliptic flow v_2 and higher correlations in high-energy high-multiplicity pp events may indicate which configurations of effective quarks and gluons in the proton structure are most likely to occur. Namely, only the **YY** configurations lead to ϵ_2 and ϵ_3 that do not fall off for N exceeding about 100. Actually, recent data [2] from ATLAS Collaboration for pp collisions with $\sqrt{s} \sim 13$ TeV show that v_2 is stable for large N. According to our analysis, this finding favors the configuration **YY**.

It should be observed that the long-range, near-side angular correlations in pp collisions at LHC energies can also be studied in terms of multiparton interactions [27]. Interactions of four partons to four partons and beyond allow for linking the ridge effect to the models [28] and theory [29] of double parton distributions and their light-front analysis [30]. A unified approach is hence greatly desired.

4 Conclusion

Simple model estimates suggest that the correlations among final-state particles in high-energy high-multiplicity pp collisions are sensitive to the proton structure. It is not excluded that future sophisticated calculations will identify some spatial features of protons through precise interpretation of experimental data on these correlations. The multidimensional linear relationship between initial-state asymmetries and final-state flow parameters that we assume in our estimates requires verification, e.g., in the hydrodynamic model. If confirmed, it would provide an efficient way for studying the proton structure through correlations in high-

multiplicity pp collisions using the universal matrices determined by the nature of assumed underlying collision dynamics. Interpreting the most recent LHC data on multiplicity dependence of the elliptic flow coefficient v_2 using our simple estimates, suggests that protons may often occur in the configuration of three effective quarks connected by a Y-shaped gluon junction.

References

1. CMS Collaboration: Observation of long-range, near-side angular correlations in proton-proton collisions at the LHC. J. High Energy Phys. **1009**, 091 (2010)
2. ATLAS Collaboration: Observation of long-range elliptic anisotropies in $\sqrt{s} = 13$ and 2.76 TeV pp collisions with the ATLAS detector (2015). arXiv:1509.04776 [hep-ex]
3. Białkowska, H.: The ridge effect from pp to Pb-Pb (and back). Acta Phys. Pol. B **43**, 705 (2012)
4. Li, W.: Observation of a Ridge correlation structure in high multiplicity proton-proton collisions: a brief review. Mod. Phys. Lett. A **27**, 1230018 (2012)
5. Bożek, P.: Elliptic flow in proton–proton collisions at sqrt(s) = 7 TeV. Eur. Phys. J. C **71**, 1530 (2011)
6. d'Enterria, D., et al.: Estimates of hadron azimuthal anisotropy from multiparton interactions in proton-proton collisions at sqrt(s) = 14 TeV. Eur. Phys. J. C **66**, 173 (2010)
7. Casalderrey-Solana, J., Wiedemann, U.A.: Eccentricity fluctuations make flow measurable in high multiplicity p–p collisions. Phys. Rev. Lett. **104**, 102301 (2010)
8. Prasad, S.K., et al.: Elliptic flow (v_2) in pp collisions at energies available at the CERN large Hadron Collider: hydrodynamical approach. Phys. Rev. C **82**, 024909 (2010)
9. Bożek, P.: Observation of the collective flow in proton-proton collisions. Acta Phys. Pol. B **41**, 837 (2010)
10. Ortona, G., et al.: Elliptic flow in high multiplicity proton-proton collisions at sqrt(s) = 14 TeV as a signature of deconfinement and quantum energy density fluctuations (2009). arXiv:0911.5158 [hep-ph]
11. Pierog, T., et al.: Collective flow in (anti)proton-proton collision at Tevatron and LHC (2010). arXiv:1005.4526 [hep-ph]
12. Bautista, I., et al.: Particle production azimuthal asymmetries in a clustering of color sources model. J. Phys. G **37**, 015103 (2010)
13. Avsar, E., et al.: Eccentricity and elliptic flow in proton-proton collisions from parton evolution. Phys. Lett. B **702**, 394 (2011)
14. Deng, W.T., et al.: Elliptic and triangular flow and their correlation in ultrarelativistic high multiplicity proton proton collisions at 14 TeV. Phys. Lett. B **711**, 301 (2012)
15. Drescher, H.J., et al.: The centrality dependence of elliptic flow, the hydrodynamic limit, and the viscosity of hot QCD. Phys. Rev. C **76**, 024905 (2007)
16. Alver, B., Roland, G.: Collision geometry fluctuations and triangular flow in heavy-ion collisions. Phys. Rev. C **81**, 054905 (2010)
17. Bjorken, J.D., et al.: Possible multiparticle ridge-like correlations in very high multiplicity proton–proton collisions. Phys. Lett. B **726**, 344 (2013)
18. Bjorken, J.D.: Double diffraction at zero impact parameter. Int. J. Mod. Phys. A **29**, 1446006 (2014)
19. Głazek, S.D.: Hypothesis of quark binding by condensation of Gluons in Hadrons. Few-Body Syst. **52**, 367 (2012)
20. Gómez-Rocha, M., Głazek, S.D.: Asymptotic freedom in the front-form Hamiltonian for quantum chromodynamics of gluons. Phys. Rev. D **92**, 065005 (2015)
21. Kubiczek, P., Głazek, S.D.: Manifestation of proton structure in the initial-state anisotropies in high-energy proton-proton collisions. Lith. J. Phys. **55**, 155 (2015)
22. Kubiczek, P.: Geometrical model of azimuthal correlations in high-multiplicity proton-proton collisions. Bachelor thesis, University of Warsaw, September (2014)
23. Miller, M.L., et al.: Glauber modelling in high energy nuclear collisions. Ann. Rev. Nucl. Part Sci. **57**, 205 (2007)
24. Blaizot, J.P., et al.: Correlations in the Monte Carlo Glauber model. Phys. Rev. C **90**, 034906 (2014)
25. CMS Collaboration: Measurement of the inelastic protonproton cross section at sqrt(s) = 7 TeV. Phys. Lett. B **722**, 5 (2013)
26. CMS Collaboration: Charged particle multiplicities in pp interactions at sqrt(s) = 0.9, 2.36 and 7 TeV. J. High Energy Phys. **1101**, 079 (2011)
27. Alderweireldt, S., Van Mechelen, P.: Obtaining the CMS ridge effect with multiparton interactions (2012). arXiv:1203.2048 [hep-ph], http://inspirehep.net/record/1093441
28. Broniowski, W., Ariola, E.R.: Valon model for double parton distributions. Contribution to LC2015 (2015)
29. Gaunt, J.: Theory of double parton scattering. Contribution to LC2015 (2015)
30. Rinaldi, M.: Double parton scattering and 3D proton structure: a light-front analysis. contribution to LC2015 (2015)